Physics Letters A 373 (2009) 1185–1188

Contents lists available at ScienceDirect

Physics Letters A

www.elsevier.com/locate/pla

Lasing of whispering-gallery modes in asymmetric waveguide GaInP micro-disks with InP quantum dots

Y. Chu [a,*], A.M. Mintairov [b], Y. He [b], J.L. Merz [b], N.A. Kalyuzhnyy [c], V.M. Lantratov [c], S.A. Mintairov [c]

[a] Department of Physics, University of Notre Dame, Notre Dame, IN 46556, USA
[b] Department of Electrical Engineering, University of Notre Dame, Notre Dame, IN 46556, USA
[c] Ioffe Physical Technical Institute, St. Petersburg, Russia

ARTICLE INFO

Article history:
Received 5 December 2008
Received in revised form 2 February 2009
Accepted 5 February 2009
Available online 13 February 2009
Communicated by R. Wu

ABSTRACT

Using wafer bonding (WB) and wet oxidation (WO) techniques, GaInP microdisks having an asymmetric waveguide (diameters $D = 1$–3 μm) with embedded InP quantum dots (size/density ∼100 nm/∼10^9 cm^{-2}) have been fabricated on Si and GaAs substrates, respectively. The $TE_{m,l}$ ($m = 28$–12, $l = 1, 2$) and $TM_{m,l}$ ($m = 25$–10, $l = 1$–4) whispering gallery modes with quality factors $Q \sim 2$–5×10^3 have been identified in photoluminescence spectra of these microdisks (MDs) in the spectral range 720–770 nm. Lasing thresholds of 6 (30) μW and mode coupling constants 0.9 (0.7) have been demonstrated for WO (WB) MDs.

Whispering-gallery-mode (WGM) semiconductor microdisk (MD) resonators with embedded quantum dots (QDs) are interesting for the realization of low threshold lasers [1,2] and for solid-state cavity quantum electrodynamics (CQED) experiments [3,4]. Up to now the most studied are GaAs MDs with InAs and InGaAs QDs emitting from 900 to 1300 nm [1–3,5–9]. For these MDs quality factors (Q) as high as 10^5 have been achieved for fundamental WGMs and room temperature lasing thresholds as low as 1 μW has been demonstrated [8]. High Q ($\sim 10^4$) MDs with GaAs/AlGaAs QDs were used to observe large (400 μeV) Rabi splitting (strong coupling regime of CQED) in low temperature emission spectra [4]. Recently, blue-green CdSe/ZnSe MDs lasers emitting at 520 nm were reported having $Q \sim 2000$ and lasing threshold ∼20 μW at room temperature [10]. Silicon based MDs with Ge QDs emitting in the range 1200–1600 nm have also been reported [11]. To date, much less work has been reported on GaInP MDs with embedded InP QDs, which offer emission wavelength 700–800 nm. Depending on the growth process, the lateral size and density of InP/GaInP QDs can have values ∼20 nm and $\sim 5 \times 10^{10}$ cm^{-2} [12,13] or ∼100 nm and $\sim 10^9$ cm^{-2} [14,15]. Larger dots are favorable for CQED experiments [4,16] or single dot lasers [6] since the coupling of the cavity mode to the emission transition and gain are proportional to dot size. We are aware of only one report on the fabrication on GaInP MDs with InP QDs, [17] in which, however, no clear WGM in the QD emission spectral range was reported, and lasing was observed only for a wetting layer at 650 nm and at temperatures below 40 K.

In the present Letter we used an InP/GaInP QD waveguide structure having lateral dot size 100 nm and density 5×10^9 cm^{-2} to fabricate microdisks emitting at ∼750 nm. Asymmetric waveguide MDs having diameters $D = 1$–4 μm were fabricated on Si and GaAs substrates using wafer bonding (WB) or wet oxidation (WO) techniques, respectively. Quality factors $Q \sim 2$ and 5×10^3 have been achieved for $TE_{m,1}$ ($m = 14$–28) modes in WB and WO disks, respectively. Lasing thresholds of 6 μW and 30 μW have been demonstrated and mode coupling constants 0.9 and 0.7 have been measured for $TE_{21,1}$ mode at room temperature in WO and WB disks.

Experimental details. Our samples were prepared from a 150 nm thick GaInP waveguide structure with embedded self-organized InP quantum dots (QDs) grown by Metal-Organic Chemical Vapor Deposition (MOCVD). The structures have been grown in a horizontal AIX200/4 reactor under pressure of 100 mbar. Initially a 700 nm thick AlAs layer was deposited on the GaAs wafer. Then a 150 nm thick $Ga_{0.52}In_{0.48}P$ waveguide layer lattice-matched to GaAs was grown with InP QDs at the center. The QDs were grown at 725 °C by depositing 7 monolayers of InP, which results in room temperature emission at 750 nm [18]. The dot density (1–5×10^9 cm^{-2}) and their sizes (∼100 nm) were estimated on uncapped samples using atomic force microscopy (AFM). The dot density of the waveguide structures was measured by near-field optical scanning microscopy [19]. The photoluminescence (PL) spectra of the InP QD ensemble shows a peak at 750 nm and half width of about 30 nm.

Microdisks having $D = 1, 1.5, 2, 2.5$ and 4 μm were fabricated using electron beam lithography (EBL) and inductively-coupled plasma reactive ion etching (ICP-RIE) by using either a wafer bonding (WB) or a wet oxidation (WO) technique. In the case of WB,

* Corresponding author.
E-mail address: ychu@nd.edu (Y. Chu).

0375-9601/$ – see front matter
doi:10.1016/j.physleta.2009.02.003

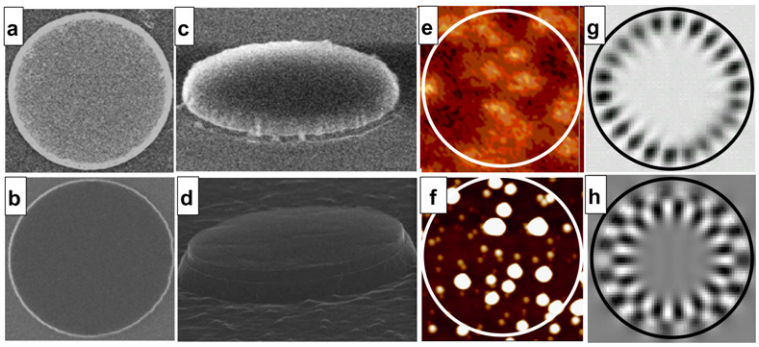

Fig. 1. Top ((a), (b)) and side ((c), (d)) view SEM images of WB ((a), (c)) and WO ((b), (d)) GaInP microdisk ($D = 2$ μm); 2×2 μm near-field image of an unprocessed wafer (e) and 2×2 μm AFM image of uncapped structure (f); Circles in (e) and (f) have diameter of 2 μm. FDTD calculated field patterns for $TE_{21,1}$ (intensity) and $TM_{15,2}$ (amplitude) WGM for $D = 2$ μm MD (g) and (h).

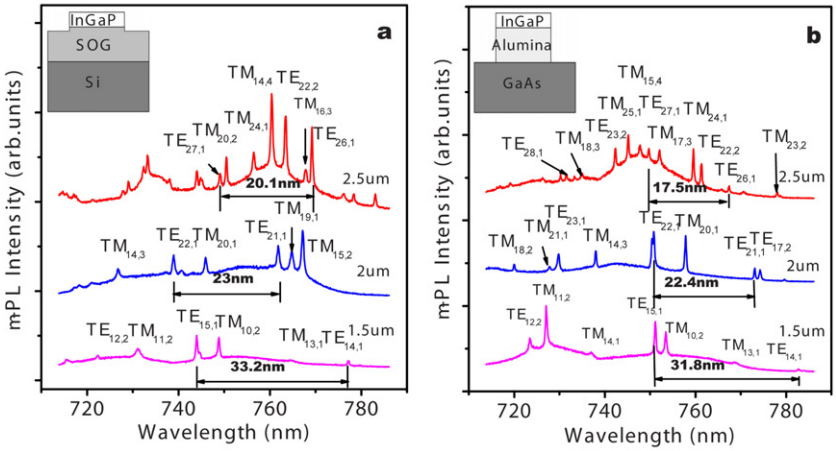

Fig. 2. Room temperature μ-PL spectra of WB (a) and WO (b) MDs having $D = 1.5, 2$ and 2.5 μm. Insets are a cartoon showing the cross section of MD structures.

the waveguide was first wafer-bonded to a Si wafer using a spin-on-glass (SOG) precursor (Filmtronics, Inc.) solution, then the GaAs substrate and the AlAs sacrificial layer were removed by mechanical polishing and chemical etching. Finally the MDs were prepared from this structure using EBL and ICP-RIE. Using the second technique, wet oxidation (WO), the MDs were formed by EBL and ICP-RIE on the initial wafer, and then the processed structure was laterally selectively-wet-oxidized to transform the AlAs layer into Al_2O_3. In Fig. 1(a), (b), (c), (d), we show scanning electron microscopy (SEM) images of 2 μm WB ((a), (c)) and WO ((b), (d)) disks from the top ((a), (b)) and side ((c), (d)). We should point out that our GaInP MDs have an asymmetric-waveguide design in both cases, as in the reference [9]. The resultant structure differs from the mushroom-like structure usually appearing in the literature, where the MD sits atop a thin pedestal to isolate it from the substrate. In our case the MD is isolated from the substrate by a low index silicate SOG ($n = 1.35$) or Al_2O_3 ($n = 1.6$) layer resulting in MDs having lower energy loss and more stable structure.

Micro-photoluminescence (μ-PL) spectra were measured using a 550 mm focal length spectrometer with a liquid-nitrogen-cooled CCD detector. The samples were excited and imaged through a home-made imaging module, consisting of a micro-objective (0.45 NA), beam-splitter and Olympus microscope illuminator with a CCD camera. The spectra were excited by 488 nm from an Ar ion laser. The effective pumping power was estimated from the disk thickness $d = 0.15$ μm, reflectivity at the disk surface $R \approx 30\%$, absorption coefficient inside the disk $\alpha \approx 46\,700\ \mathrm{cm}^{-1}$ which is calculated from Kurtz's model [20], and the multiple absorption in the disk expressed as $(1 - R)(1 - e^{-\alpha d})/(1 - Re^{-\alpha d})$ [21]. The absorption efficiency of the pumping laser is estimated to be 42%. With this efficiency, the measured pumping power is converted into efficient pumping power, P_{eff}, as shown in figures included in this Letter. Time-resolved measurements were done with a streak camera (time resolution 4 ps) coupled to the same monochromator under 400 nm excitation from a frequency doubled Ti:sapphire laser.

The calculations of mode frequencies and field/intensity distributions, which allow the identification of mode polarization (TE or TM) and azimuthal (m) and radial (l) numbers, were done using 3D finite-difference-time-domain (FDTD) commercial software by Lumerical Inc. The calculation details can be found in our previous work [19].

A near-field optical scanning microscopy image of unprocessed wafer (detection wavelength 750 nm) and AFM image of an uncapped structure are shown for scan area 2×2 μm in Fig. 1(e) and (f). Field intensity and amplitude patterns of the $TE_{21,1}$ and $TM_{15,2}$ WGMs, respectively, calculated by FDTD for a $D = 2$ μm MD are shown in Fig. 1(g) and (h). As can be seen in both (e) and (f), only a few QDs spatially overlap with the mode pattern, which means that the WGMs were generated by just a few QDs, or even a single QD.

Results. Fig. 2(a) and (b) show the μ-PL spectra from MDs having $D = 1.5, 2, 2.5$ μm on both WB and WO structures. The sharp lines denoted as $TE_{m,l}$ and $TM_{m,l}$ are whispering gallery modes. One can see that the number of the sharp lines increases as the MD diameter increases. The azimuthal and lateral number of WGMs have been assigned to each line according to FDTD calculations. We can see the following dominant modes in the spectral range 710–790 nm: for the MD with $D = 2.5$ μm, fundamental modes $TE_{m,1}$ ($m = 26$–28), $TM_{m,1}$ ($m = 24, 25$); for the $D = 2$ μm MD, $TE_{m,1}$ ($m = 21$–23), $TM_{m,1}$ ($m = 19, 20$) and for the $D = 1.5$ μm

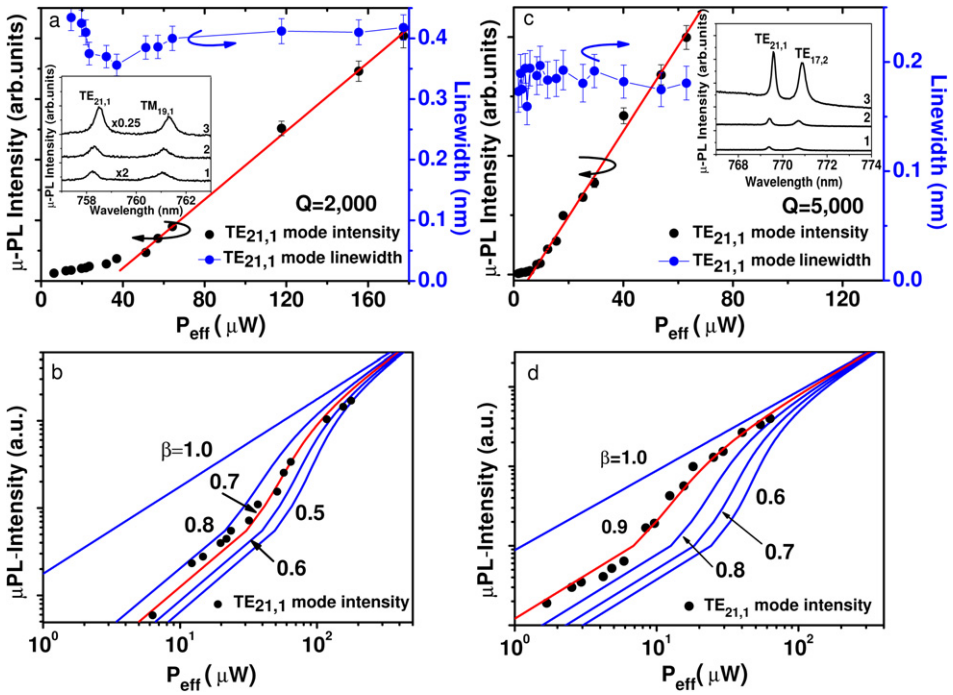

Fig. 3. (a) and (c) show intensity (left y-axis) and linewidth (right y-axis) versus pump power of whispering gallery mode $TE_{21,1}$ for WB and WO MDs ($D = 2$ μm) in linear scale; (b) and (d) show the intensity versus pump power in logarithmic scale. Insets in (a) and (c) are the μ-PL spectra taken at pump powers: 15, 24 and 64 μW (a) and 12, 20 and 57 μW (c) for spectra 1, 2 and 3, respectively. The solid lines are the fitting curves.

MD, $TE_{m,1}$ ($m = 14, 15$), and $TM_{m,1}$ ($m = 13, 14$). The higher order modes are $TE_{m,2}$ ($m = 22, 23$), $TM_{m,2}$ ($m = 20, 23$), $TM_{m,3}$ ($m =$ 16–18), $TM_{m,4}$ ($m = 14, 15$) for $D = 2.5$ μm MD; $TE_{17,2}$, $TM_{m,2}$ ($m = 10, 11$), $TM_{14,3}$ for $D = 2$ μm MD; $TE_{12,2}$, $TM_{m,2}$ ($m = 10, 11$) for $D = 1.5$ μm MD. Because of the larger refractive index of Al_2O_3 compared to SOG, WO MDs have larger optical volume, which results in longer WGM mode wavelength and smaller free spectral range (FSR, the spacing between modes). One can see that for $D = 2$ μm, the $TE_{21,1}$ WGM has wavelength 758 and 770 nm, for WB and WO, respectively, and that for $D = 2.5$ μm WO MD has a FSR of 18 nm while the WB one has 20 nm, also shown in Fig. 2). WO MDs generally have a higher Q-factor than the WB MDs (cf. Fig. 3). This is due to the wafer bonding process which introduces more defects, such as surface strain, surface roughness and disk region tilting. However, the wafer bonded MD will have its advantages of using Si (or any other) substrates.

Fig. 3(a) and (c) show the intensity and spectral linewidth versus pump power of WGM $TE_{21,1}$ for WB and WO MDs ($D = 2$ μm) in linear scale, and Fig. 3(b) and (d) show the intensity versus pump power in logarithmic scale. Insets in (a) and (c) are the μ-PL spectra taken at pump powers: 15, 24 and 64 μW (a) and 12, 20 and 57 μW (c) for spectra 1, 2 and 3, respectively. Dots are experimental data points, solid lines are the fitting curves. Lasing was identified as a sharp change of slope of the intensity versus power curve in the linear scale (see Fig. 3(a) and (c)). Lasing was observed for $TE_{21,1}$ and $TM_{15,2}$ modes with a $Q = 2100$ and 1900 at 758 nm and 761 nm, respectively, in the WB MD. In the WO MD, lasing was observed for $TE_{21,1}$ and $TM_{20,1}$ with $Q = 5000$ and 2500 at 770 nm and 771 nm. (Note that the TM modes are not shown in Fig. 3.) The threshold power for $TE_{21,1}$ mode was measured to be 30 and 6 μW for WB and WO MD, respectively. This corresponds to power density 955 $W\,cm^{-2}$ and 190 $W\,cm^{-2}$. The lower threshold power for WO MD is well accounted for by the higher Q value. We believe that this is the first observation of room-temperature CW optically-pumped lasing in InP QD MDs. The spectral linewidth of the lasing mode of WB MD shows clear drop from 0.45 to 0.36 nm near the threshold. On the other hand, for WO MD we will no be able to reveal clear drop of the mode width, having value 0.18 nm. This indicates different absorption losses in WB and WO MDs, which are directly related to number of QDs coupled to WGM. This shows that in our MD we have few or only a single QD lased.

One can derive the relationship between the emitted intensity and the excitation power for semiconductor lasers theoretically as: $I = \frac{q\gamma}{\beta}[\frac{p}{1+p}(1+\xi)(1+\beta p) - \xi\beta p]$ [22] where I is the excitation current, p is the number of photons in the mode. For optical excitation, I corresponds to the pumping power and p is proportional to the output intensity. γ is the cavity decay rate, and β describes the fraction of the spontaneous emission that is coupled into the lasing mode. ξ is the ratio of spontaneous photon emission into the lasing mode and the cavity decay rate, and it is defined as: $\xi = \frac{N_0\beta V}{\gamma\tau_{sp}}$, where N_0 is the transparency carrier concentration of the gain material, V is the volume of active material, and τ_{sp} is the spontaneous lifetime of the active material when it sits in a cavity. When β is small, a sharp threshold for lasing is expected, when β is large (close to unity), we can expect a very low lasing threshold. Our measured data can be fitted well with $\beta = 0.7$ and 0.9, $\xi = 42$ and 90 for WB and WO MD, respectively, as shown in Fig. 3(b), (d). The carrier density N_0 calculated from the fitting parameter ξ[1] is 11.2×10^9 cm^{-2} and 7.2×10^9 cm^{-2} for WB and WO MD, respectively, which is 2 and 1.5 times higher than the QD density estimated from the AFM image (5×10^9 cm^{-2}). This means that we have more than one electron from a single QD. The predicted Purcell factor, $F_p = \frac{3}{4\pi^2}(\frac{\lambda_c}{n})^3(\frac{Q}{V_{eff}})$ [23], for WB MD is ~25.3 and for WO MD is ~63.4. Taking into account the two-fold degeneracy of the mode, the spectral and spatial averaging, and the random dipole orientation, we can calculate the average spontaneous emission enhancement from $\frac{\gamma}{\gamma_0} = \frac{Q\lambda^3}{2\pi^2 n^3 V_{eff}}\frac{\Delta\lambda^2}{\Delta\lambda^2+4(\lambda_e-\lambda)^2} + f = \frac{2F_p}{2\cdot 2\cdot 3} + 1$ [23,24]. The calculated $\beta = 1 - \frac{\gamma_0}{\gamma} = 0.8$ and 0.91, for WB and WO

[1] We used $\tau_{sp} = 8$ ps, this value was obtained from the measured value of 10 ps and it is accounted for the instrumental response of our setup.

MD, respectively. Thus, the spontaneous emission rate β we got from simulation using rate equation (0.7 and 0.9) is consistent with the one calculated from Purcell factor (0.8 and 0.91).

In conclusion, whispering gallery modes and low-threshold room-temperature lasing have been observed from phosphide-based semiconductor microdisks for the first time. These MD structures ($D = 1$–4 μm) with InP/GaInP QDs (lateral size 100 nm and density 5×10^9 cm^{-2}) have been fabricated from asymmetric air/GaInP/SOG and air/GaInP/Al_2O_3 waveguides on Si and GaAs substrates, using wafer bonding (WB) and wet oxidation (WO) techniques, respectively. Quality factors $Q \sim 2$–5×10^3 have been measured in μ-PL spectra for $TE_{m,1}$, ($m = 14$–28, $D = 2$ and 2.5 μm) modes in the spectral range 720–780 nm. Lasing thresholds 6 and 30 μW have been demonstrated and mode coupling constants 0.9 and 0.7 have been measured for the $TE_{21,1}$ mode at room temperature in WO and WB disks, respectively.

Acknowledgements

We wish to acknowledge NSF MRI grant DMR 06-19725 for the streak camera used for the time-resolved measurements, NSF NIRT grant ECS-0609249 for NSOM measurements and NSF FRG grant DMR 06-06406 for support of one of the authors (Y.H.).

References

[1] H. Cao, J.Y. Xu, W.H. Xiang, Y. Ma, S.-H. Chang, S.T. Ho, G.S. Solomon, Appl. Phys. Lett. 76 (2000) 3519.
[2] P. Michler, A. Kiraz, L. Zhang, C. Becher, E. Hu, A. Imamoglu, Appl. Phys. Lett. 77 (2000) 184.
[3] A. Kiraz, P. Michler, C. Becher, B. Gayral, A. Imamoglu, L. Zhang, E. Hu, W.V. Schoenfeld, P.M. Petroff, Appl. Phys. Lett. 78 (2001) 3932.
[4] E. Peter, P. Senellart, D. Martrou, A. Lemaître, J. Hours, J.M. Gérard, J. Bloch, Phys. Rev. Lett. 95 (2005) 067401.
[5] K.J. Luo, J.Y. Xu, H. Cao, Y. Ma, S.H. Chang, S.T. Ho, G.S. Solomon, Appl. Phys. Lett. 78 (2001) 3397.
[6] Z.G. Xie, S. Götzinger, W. Fang, H. Cao, G.S. Solomon, Phys. Rev. Lett. 98 (2007) 117401.
[7] S.A. Blokhin, N.V. Kryzhanovskaya, A.G. Gladyshev, N.A. Maleev, A.G. Kuzmenkov, E.M. Arakcheeva, E.M. Tanklevskaya, A.E. Zhukov, A.P. Vasiĭev, E.S. Semenova, M.V. Maximov, N.N. Ledentsov, V.M. Ustinov, E. Stock, D. Bimberg, Phys. Semiconduct. Devices 40 (2005) 476.
[8] K. Srinivasan, M. Borselli, O. Painter, A. Stintz, S. Krishna, Opt. Express 14 (2006) 1094.
[9] E. Peter, I. Sagnes, G. Guirleo, S. Varoutsis, J. Bloch, A. Lemaître, P. Senellart, Appl. Phys. Lett. 86 (2005) 021103.
[10] J. Renner, L. Worschech, A. Forchel, S. Mahapatra, K. Brunner, Appl. Phys. Lett. 89 (2006) 231104.
[11] J.S. Xia, K. Nemoto, Y. Ikegami, Y. Shiraki, N. Usami, Appl. Phys. Lett. 91 (2007) 011104.
[12] T. Riedl, E. Fehrenbacher, A. Hangleiter, M.K. Zundel, K. Eberl, Appl. Phys. Lett. 73 (1998) 3730.
[13] A. Moritz, R. Wirth, A. Hangleiter, A. Kurtenbach, K. Eberl, Appl. Phys. Lett. 69 (1996) 212.
[14] D.A. Vinokurov, V.A. Kapitonov, D.N. Nikolaev, Z.N. Sokolova, I.S. Tarasov, Semiconductors 35 (2) (2001) 235.
[15] M.-E. Pisto, J. Phys.: Condens. Matter 16 (2004) S3737.
[16] G. Sek, C. Hofmann, J.P. Reithmaier, A. Löffler, S. Reitzenstein, M. Kamp, L.V. Keldysh, V.D. Kulakovskii, T.L. Reinecke, A. Forchel, Physica E 32 (2006) 471.
[17] V. Zwiller, S. Fälth, J. Persson, W. Seifert, L. Samuelson, G. Björk, J. Appl. Phys. 93 (2003) 2307.
[18] D.A. Vinokurov, V.A. Kapitonov, O.V. Kovalenkov, D.A. Livshits, I.S. Tarasov, Tech. Phys. Lett. 24 (1998) 623.
[19] A.M. Mintairov, Y. Chu, Y. He, S. Blokhin, A. Nadtochy, M. Maximov, V. Tokranov, S. Oktyabrsky, J.L. Merz, Phys. Rev. B. 77 (2008) 195322.
[20] S.R. Kurtz, J.M. Olson, K. Bertness, D.J. Friedman, J.F. Geisz, A.E. Kibbler, presented at Materials Research Society's Spring Meeting, San Francisco, California (1999).
[21] K. Nozaki, A. Nakagawa, D. Sano, T. Baba, IEEE J. Sel. Top. Quantum Electron. 9 (2003) 1355.
[22] G. Björk, Y. Yamamoto, IEEE J. Quantum Electron. 27 (1991) 2386.
[23] J.M. Gérard, B. Gayral, J. Lightwave Technol. 17 (1999) 2089.
[24] G.S. Solomon, M. Pelton, Y. Yamamoto, Phys. Rev. Lett. 86 (2001) 3903.